Proc. Natl. Acad. Sci. USA
Vol. 79, pp. 4461–4465, July 1982
Neurobiology

Electron microscopic visualization of the tetrodotoxin-binding protein from *Electrophorus electricus*

(saxitoxin/sodium channel/action potential/negative staining/electrical excitability)

M. H. ELLISMAN*, W. S. AGNEW†, J. A. MILLER†, AND S. R. LEVINSON‡

*Department of Neurosciences, School of Medicine, University of California at San Diego, La Jolla, California 92093; †Department of Physiology, Yale University, New Haven, Connecticut 06510; and ‡Department of Physiology, University of Colorado Medical School, Denver, Colorado 80262

Communicated by Theodore H. Bullock, April 19, 1982

ABSTRACT **Preparations of highly purified tetrodotoxin-binding protein (sodium channel) from the electric organ of the eel *Electrophorus electricus* were examined in negatively stained preparations. Structures observed in preparations exhibiting the highest tetrodotoxin binding tended to aggregate into ordered clusters with a unique ribbon-like conformation. The individual particles of these aggregates are elongated or rod-shaped, approximately 40 Å wide and 170 Å long. Stereoscopic imaging of the three-dimensional aspects of the structures revealed that the rod-like image is not an edge view of a flattened disc but represents a cylindrical structure. Individual rods in nonclustered forms were also observed but with greater frequency in preparations with lower specific activity. The dimensions of the particles suggest that they represent a protein core formed by perhaps one copy of the large glycopeptide previously identified as being part of the sodium channel. The structure of the sodium channel component visualized by negative staining is discussed in the context of the excitable properties it contributes to biological membranes.**

The electrical excitability of the membranes of both nerve and muscle cells is a consequence of rapid and precisely controlled changes in the membrane conductance of specific ions, notably Na^+ and K^+. The electrical potential across the membrane is a consequence of the relative permeabilities to these ions (1–3), which are, in turn, modulated by the action of highly specialized ion channels (4, 5). Electrophysiological and pharmacological properties of the channels have been well studied (6, 7), but little is known of the structural and mechanistic characteristics of these complex protein structures (4, 5). Indeed, these "electrically excitable channels" represent a previously uncharacterized class of membrane proteins. The voltage-sensitive sodium channel forms a cation-selective pore that spans the membrane and transports sodium in preference to other ions present in physiological solutions (8). This channel is gated by the transmembrane voltage to a sequence of resting, open, and closed states during excitation, thus resulting in a transiently open pore (1, 2).

There are a variety of pharmacological agents that interfere with the complex function of the sodium channel. Among these, the neurotoxins tetrodotoxin (TTX) and saxitoxin reversibly block sodium movement at nanomolar concentrations, apparently by occluding the pathway through which the ions pass (9). The remarkable specificity of these toxins has resulted in their application as biochemical markers for quantitation of the sodium channel in tissues, disrupted membranes, and solubilized preparations (6, 10).

We have been engaged in the biochemical isolation of the voltage-sensitive sodium channel from the electroplax of the South American eel *Electrophorus electricus*. We have previously described the purification of the TTX- and saxitoxin-binding protein from the electroplax membrane and some of its physicochemical characteristics (11). It is a glycoprotein of $s_{20,w}$ = 8 S and Stokes radius = 95 Å, and, purified, it is an aggregate particle of protein–detergent (Lubrol-PX) and phospholipid (phosphatidylcholine). The principal and perhaps sole peptide component of the molecule is one or more large glycopeptides of nominal molecular weight of 260,000 by $NaDodSO_4$ gel electrophoresis (11). It has been possible to obtain this material in 0.1- to 1.0-mg amounts by relatively simple methods (12). The present report describes the appearance of the purified solubilized TTX-binding protein (TTXR, TTX receptor) by electron microscopy, using the technique of negative staining.

METHODS

TTXR Purification. Citrate-free TTX was the kind gift of Y. Kishi (Harvard University). The toxin was tritiated by the Wilzbach procedure and purified from radioactive contaminants by ion-exchange chromatography (13). The purified toxin was approximately 65% pure as determined by the frog sciatic nerve bioassay (14) and was of specific activity 58.6 Ci/mol (1 Ci = 3.7×10^{10} becquerels). TTX-binding assays were done by the Sephadex G-50 assay of Levinson *et al.* (15).

$NaDodSO_4$/polyacrylamide gel electrophoresis was performed by the method of Laemmli (16), using gels of 6% acrylamide/0.8% bisacrylamide. Protein was estimated by the fluorescence procedure (17), with bovine serum albumin as a standard.

The purification of the TTXR was similar to that reported by Agnew *et al.* (18). Medium-sized eels (1–1.5 m) were killed by hypothermia, and the main organs were removed and stored at −80°C. Partially thawed organs were then trimmed of connective tissue, cut into 1- to 2-cm slices, and placed in a beaker with 4 vol of 0.05 M potassium phosphate buffer (pH 6.8), 0.1 mM phenylmethylsulfonyl fluoride, and 5 mM Na_2EDTA and were homogenized for 30 sec with a Tekmar SD-45 homogenizer at full speed. The homogenate was strained through two layers of cheesecloth and centrifuged in the JA14 rotor of the Beckman J2-21 centrifuge at 14,000 rpm for 20 min. The supernatant was discarded. The pellets were pooled and added to an equal weight of buffer. Samples were shaken vigorously to form a homogeneous suspension, which was then placed in 50-ml tubes of a JA20 rotor and centrifuged for 60 min at 20,000 rpm. Supernatants were discarded and the pellets were weighed. Pellets were resuspended in an equal volume of the buffer with low-speed homogenization and portions were put into plastic vials for storage at −80°C.

The publication costs of this article were defrayed in part by page charge payment. This article must therefore be hereby marked "*advertisement*" in accordance with 18 U. S. C. §1734 solely to indicate this fact.

Abbreviations: TTX, tetrodotoxin; TTXR, TTX-binding protein (TTX receptor).

For purification, 50–80 ml of membranes was thawed, made to 1% (wt/vol) with Lubrol-PX, gently homogenized with a Potter–Elvehjem homogenizer, and placed in the tubes of a Beckman 40Ti rotor. The samples were centrifuged at 40,000 rpm for 1 hr in a Beckman L2-65 ultracentrifuge. The supernatants were pooled and assayed for TTX-binding activity and protein. They were then made 0.2 M in KCl and added to an equal volume of DEAE-Sephadex A-25 (Pharmacia), previously equilibrated with 0.2 M KCl/0.05 M potassium phosphate buffer at pH 6.8 and 0.1% Lubrol-PX/phosphatidylcholine, 7:1 (mol/mol). After 30-min equilibration at ice-bath temperatures, the gel was sedimented and the supernatant was discarded. The gel was washed at least five times with an equal volume of 0.2 M KCl in the same buffer. The gel was then mixed with an equal volume of 0.6 M KCl in the buffer. After 30 min the gel was pelleted and the supernatant was removed. The gel was quickly washed with an additional 0.5 vol of 0.4 M KCl in the same buffer. The two supernatants were pooled, made 50 nM in [^{3}H]TTX, and concentrated over an XM-300 membrane in an Amicon pressure dialyzer under 10 pounds/inch^2 (69 kPa) of N_2. The concentrate (generally less than 2 ml) was assayed for TTX-binding activity. The concentrate was supplemented with 100 μl of 0.5 M potassium phosphate buffer and 100 μl of 2.5 M [^{3}H]TTX and was delivered to a 1.6 × 65 cm column of Sepharose 6B (Pharmacia). The column had been freshly equilibrated with 0.1 M potassium phosphate buffer at pH 6.8, 0.1% Lubrol-PX/phosphatidylcholine, and 50 nM [^{3}H]TTX at 4°C. Fractions (3.25 ml) were collected and were assayed for TTX binding and protein. Samples of relevant fractions were saved for analysis by $NaDodSO_4$ gel electrophoresis. Only the highest specific activity fractions (one or two fractions) were pooled, made 100 nM in [^{3}H]TTX, and concentrated over an XM-50 membrane in an Amicon pressure dialyzer to approximately 0.5 ml. This was delivered to a second, smaller (0.5 × 45 cm) Sepharose 6B column. Fractions (0.67 ml) were collected and assayed for TTX binding and protein. The highest specific activity fractions were analyzed by $NaDodSO_4$ gel electrophoresis and were used for visualization. Samples were dialyzed for 12 hr against two changes (500 ml each) of 0.2 M $NaHCO_3$ at pH 9.0 containing 0.1% Lubrol-PX/phosphatidylcholine. Some samples were examined without dialysis (i.e., at pH 6.8). The appearance of particles under these conditions was not markedly different than under the standard conditions. All samples used for visualization had specific activities of 2,000 pmol of TTX-binding sites per mg of protein or greater.

Electron Microscopy Negative Staining. For electron microscopic visualization approximately 10 μl of the sample was applied to a carbon film on a 400 mesh copper grid (Pelco) pretreated with aqueous poly(L-lysine) hydrobromide (Sigma) at 50 μg/ml and negatively stained with 2% aqueous uranyl acetate (Polysciences). The samples were examined at 80 kV with a top-entry JEOL 100B electron microscope and a side-entry JEOL 100CX electron microscope, both equipped with specimen anticontamination devices and the 100CX with a eucentric goniometric stage.

Quantitative Analysis of Particle Size. Measurements of particle sizes were made directly on ×100, ×120, and ×130 negatives or on prints with a total magnification of 125,000–250,000, using a ×10 magnifying loupe with a graticule. Samplings of both particles in clusters and individuals were measured. Over 250 particle measurements were made, from which the average and standard deviation estimates were obtained. Tilting of rods as seen in Fig. 2*B* can foreshorten the rods' true length, but never extend it. Thus, measurements of rod length were limited to rods that were determined to be flat in the analyzed micrograph by stereoscopic viewing. The true operating magnifications of the microscopes at each indicated magnification were determined by using a calibration grid (T. Pella).

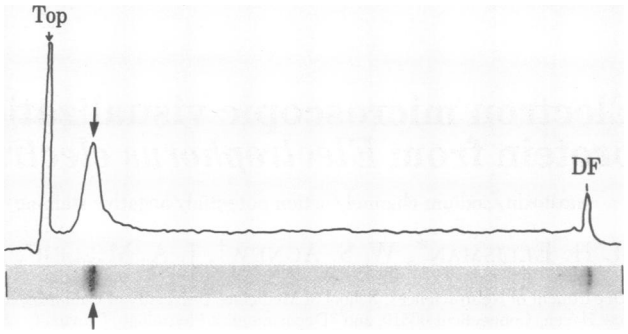

FIG. 1. Example of purified TTXR material analyzed by $NaDodSO_4$ gel electrophoresis and the associated gel scan. DF, dye front. The arrows mark the position of the major TTXR polypeptide.

RESULTS

Preparations of the TTXR used for visualization had specific activities greater than 2,000 pmol of TTX-binding sites per mg of protein, and when analyzed by $NaDodSO_4$/polyacrylamide gel electrophoresis were shown to consist almost entirely of the 260,000-dalton peptide. The samples used in the experiments illustrated here had specific activities better than 2,200 pmol of TTX bound per mg of protein. Fig. 1 shows the $NaDodSO_4$ gel and the densitometer scan of one such preparation.

In most of the fields examined at low magnification, the most distinctive structures observed were clusters of rod-shaped particles. Examples of these are shown in Fig. 2. These clusters were composed of from a few up to several hundred elongated particles often lying in register along with their long axes. The aggregates were found in all samples examined, but seemed to be more abundant in preparations of higher protein concentration and higher specific activities. The rods of the clusters had average lengths of 170 Å (SD = 6 Å; variance = 39 Å) and average widths of 41 Å (SD = 3 Å; variance = 7 Å). Stereoscopic visualization of the loose cluster of rod-shaped particles reveal that the individuals are indeed cylinders and are not discoid in shape (Fig. 2*B*). In the highest resolution micrographs some of the rod-shaped particles appeared to be segmented and possibly composed of smaller subunits (Fig. 2*C*).

Extensive examination of nonclustered material failed to reveal consistently sized particles. Many individual rod-shaped elements like those found clustered were observed. Non-rod-shaped bits of material encountered in the specimens did not exhibit a consistent size or characteristic shape, in contrast to what is found for some other membrane proteins such as the

FIG. 2 *(on following page)*. Electron micrographs of negatively stained TTXR preparations. All calibration bars represent 1,000 Å. (*A*) Field of clustered particles forming long twisting ribbons. Several well-aligned and well-contrasted stacks are denoted by arrows. (×75,000.) (*B*) Stereo pair micrographs from another preparation illustrating the ribbon-like nature of these clusters. When viewed in stereo, the twisting of these ribbons may be appreciated. Note that the large open arrows point out areas where the rods of the clusters are normal to the viewer, whereas the black arrows indicate areas where the rods are tipped up. (Stereo viewing with a two-lens viewer is recommended.) (×100,000.) (*C*) Representative images of small clusters of rods from different preparations. The small arrows point to several well-delineated structures. Note that several of the rods pointed out in the middle panel exhibit a segmented or beaded appearance not unlike a short segment of twisted rope. (×265,000.)

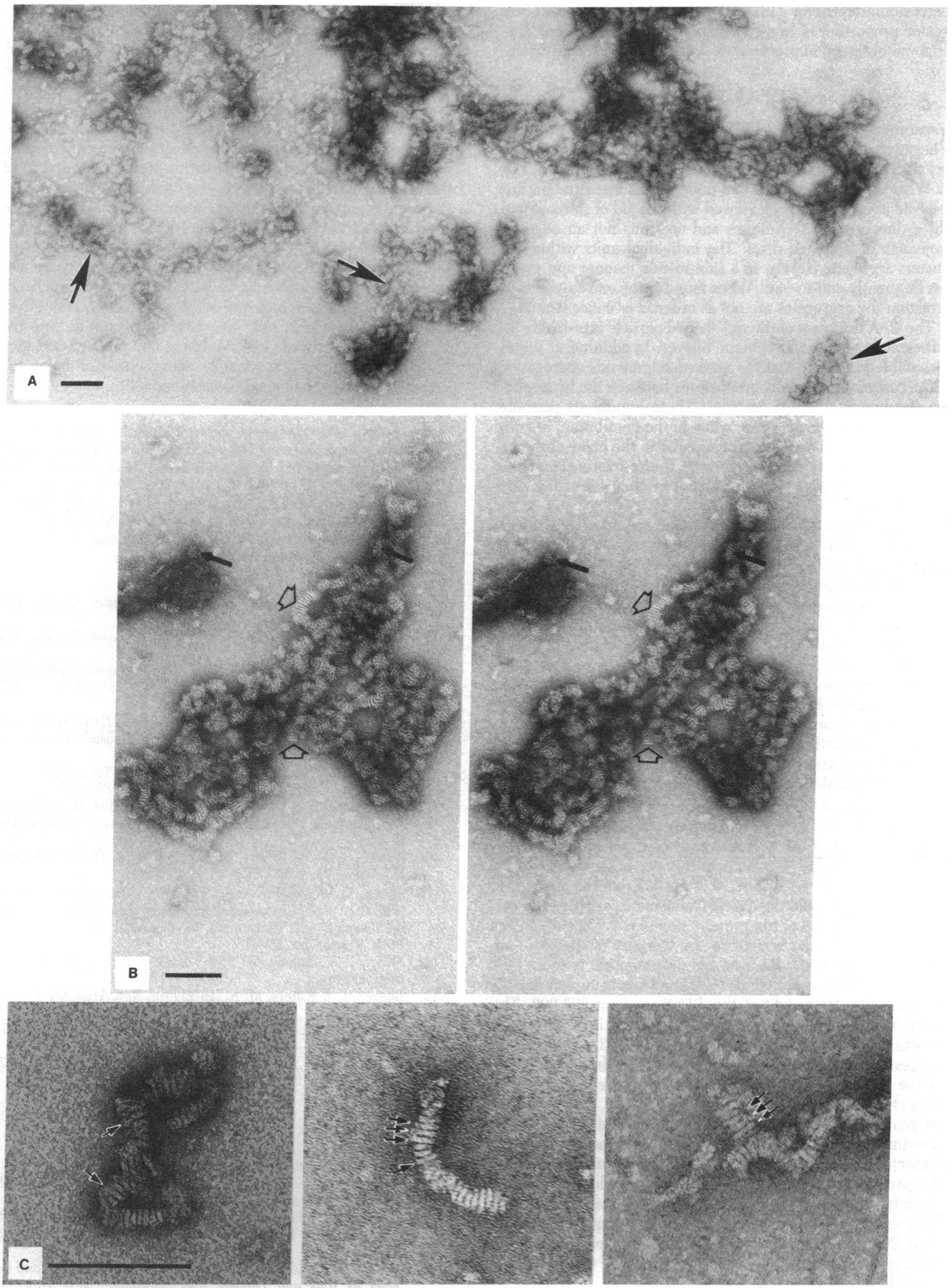

FIG. 2. *(Legend appears at the bottom of the preceding page.)*

acetylcholine receptor (19) and bacterial rhodopsin (20). A greater proportion of non-rod-shaped and non-clustered material was observed in preparations with lower specific activities.

DISCUSSION

Preparations of purified TTXR, when visualized with the aid of negative staining in the electron microscope, appear as clusters of rod-shaped particles of approximate dimensions 40 × 170 Å. What appear as rods in two-dimensional visualization are resolved as cylinders when viewed with the aid of stereoscopic (three-dimensional) techniques and are thus not an edge-on projection of flattened discs. The individual units within the clusters aggregate closely, in a side-to-side manner and much less frequently end-to-end. When found in the end-to-end confirmation the aggregates are not as ordered or concentrated.

The 40-Å thickness of the rod-shaped particle is probably insufficient to span the membrane bilayer. In addition, it seems reasonable to assume that the marked side-to-side aggregation of the particles represents interactions between the hydrophobic domains of adjacent particles. These arguments promote speculation that the particles, when in the membrane, are oriented with their long axis perpendicular to the plane of the bilayer. Attempts at correlation with freeze-fracture particles however, may support the proposal of another orientation (see the following).

It is prudent to exercise caution in interpretation of absolute sizes of the TTXR determined in these negatively stained preparations. It is unlikely that the negative staining protocols used revealed the entire molecule. It is known that this TTXR's composition is approximately 30% carbohydrate by weight (12), and the carbohydrate-rich portions most likely extend to the external surface of the membrane. The negative staining protocols used here most likely reveal the proteinaceous core in negative contrast while positively staining the carbohydrate-rich portion of the molecule. Preparative methods could alter the true molecular dimensions. Measurements of such small objects are not usually reproducible at the ångstrom level. Hence the standard deviation and variance values likely contain a small component (1–2 Å) attributable to measurement accuracy.

An estimate of the molecular size of these rods may be made by assuming a rod of 40 × 170 Å and by assuming that the image represents that of the proteinaceous core and not the carbohydrate component. A particle of this size has a volume of 2.2×10^{-19} cm^3 (SD = $\pm 0.2 \times 10^{-19}$ cm^3). From the amino acid composition (12), and the data of Cohn and Edsall (21), the partial specific volume of the protein moiety is 0.752 cm^3/g. The computed molecular weight of the cylinder is therefore approximately 180,000. Because the glycopeptide is about 70% protein and 30% carbohydrate (12) this estimate implies that the actual molecular weight of the TTXR is about 257,000. This value is in good agreement with estimates by irradiation inactivation (4) and sedimentation studies (22, 23). Further, the longest axis of the particle is consistent with the Stokes radius of the detergent-solubilized molecule measured by gel exclusion chromatography (95 Å) (18). For instance, if lipid and detergent were bound along the circumference of the rod, an approximately spherical particle of these dimensions would be expected. Miller and co-workers (12) have demonstrated that the precise molecular weight of the glycopeptide (Fig. 1) cannot be determined by NaDodSO$_4$ gel electrophoresis. Nevertheless they suggest that the true value is likely to be equal to or greater than 260,000. Thus, the values computed above suggest that each particle may be composed of one copy of the large glycopeptide.

It is noteworthy that rod-shaped particles have been observed in freeze-fracture replicas on both endoplasmic and protoplasmic fracture faces of nodes of Ranvier (24–26), which are known to contain the TTXR protein from immunocytochemical studies (27, 28). Although a direct correlation between these molecules delineated by negative staining and those exposed by freeze-fracture is attractive, it is at this time only speculative. Direct freeze-fracture visualization of purified TTXR in native or in reconstituted membranes, however, will be enlightening with respect to this possible correlation and the orientation of the irregularly shaped protein in the lipid bilayer.

Recent reports by Beneski and Catterall (29) that the peptide toxin from *Leirus* venom, which alters gating, also binds to peptides of molecular weight approximately 250,000 gives us hope that we may ultimately find that the gating elements are also represented in the molecule we have isolated and visualized. Thus, the functional complexity of the channel may result from the folding of perhaps only one large glycopeptide into the rather elaborate particle observed here and not an association of many discrete peptide subunits as in the case of the acetylcholine receptors of all species examined (30).

The authors acknowledge the expert technical assistance of Tom Deerinck on microscopes and Dolores Taitano on computer keyboard. This work was supported by grants from the National Institutes of Health to M.H.E. (NS14718) and S.R.L. (NS15879) as well as grants from the Muscular Dystrophy Association to M.H.E. and the National Multiple Sclerosis Society to W.S.A. and M.H.E. Also, M.H.E. was an Alfred P. Sloan Research Fellow while conducting this research. S.R.L. is a Research Career Development Awardee.

1. Hodgkin, A. L. & Huxley, A. F. (1952) *J. Physiol. (London)* **116**, 449–472.
2. Hodgkin, A. L. & Huxley, A. F. (1952) *J. Physiol. (London)* **116**, 473–496.
3. Hodgkin, A. L. & Katz, B. (1949) *J. Physiol. (London)* **108**, 37–77.
4. Levinson, S. R. & Ellory, J. C. (1973) *Nature (London)* **245**, 122–123.
5. Levinson, S. R. (1981) in *Molecular Basis of Drug Action*, eds. Singer, T. & Ondarza, R. (Elsevier/North-Holland, Amsterdam), pp. 315–331.
6. Catterall, W. A. (1980) *Annu. Rev. Pharmacol. Toxicol.* **20**, 15–44.
7. Armstrong, C. M. (1974) *Q. Rev. Biophys.* **7**, 179–210.
8. Hille, B. (1975) *Fed. Proc. Fed. Am. Soc. Exp. Biol.* **34**, 1318–1321.
9. Kao, C. Y. & Nishiyama, A. (1965) *J. Physiol. (London)* **180**, 50–66.
10. Ritchie, J. M. & Rogart, R. B. (1977) *Rev. Physiol. Biochem. Pharmacol.* **79**, 1–50.
11. Agnew, W. S., Moore, A. C., Levinson, S. R. & Raftery, M. A. (1981) in *Nerve Membrane: Biochemistry and Function of Channel Proteins*, eds. Matsumoto, G. & Kotani, M. (Univ. Tokyo Press, Tokyo), pp. 25–44.
12. Miller, J. A., Agnew, W. S. & Levinson, S. R. (1982) *Biochemistry*, in press.
13. Benzer, T. & Raftery, M. A. (1972) *Proc. Natl. Acad. Sci. USA* **69**, 3634–3637.
14. Levinson, S. R. (1975) *Phil. Trans. R. Soc. London Ser. B* **270**, 337–348.
15. Levinson, S. R., Curatalo, C. J., Reed, J. & Raftery, M. A. (1979) *Anal. Biochem.* **99**, 72–84.
16. Laemmli, U. K. (1970) *Nature (London)* **277**, 680–685.
17. Udenfriend, S., Stein, S., Bohlen, P., Dairman, W., Leimgruber, W. & Weigele, M. (1972) *Science* **178**, 871–872.
18. Agnew, W. S., Levinson, S. R., Brabson, J. S. & Raftery, M. A. (1978) *Proc. Natl. Acad. Sci. USA* **75**, 2606–2610.
19. Lindstrom, J., Gullick, B., Conti-Tronconi, B. & Ellisman, M. H. (1980) *Biochemistry* **19**, 4791–4795.
20. Darzon, A., Vandenberg, C. A., Schonfeld, M., Ellisman, M. H., Spitzer, N. & Montal, M. (1980) *Proc. Natl. Acad. Sci. USA* **77**, 239–243.
21. Cohn, E. J. & Edsall, J. T. (1943) *Proteins, Amino Acids and Peptides as Ions and Dipolar Ions* (Reinhold, New York), pp. 370–381.

22. Barchi, R. L. & Murphy, L. E. (1981) *J. Neurochem.* **36**, 2097–2100.
23. Hartshorne, R. P. & Catterall, W. A. (1981) *Proc. Natl. Acad. Sci. USA* **78**, 4620–4624.
24. Ellisman, M. H. (1976) *Soc. Neurosci. Abstr.* **2**, 410 (abstr.).
25. Ellisman, M. H. (1979) *J. Neurocytol.* **8**, 719–735.
26. Rosenbluth, J. (1979) *J. Neurocytol.* **5**, 731–745.
27. Ellisman, M. H., Lindsey, J. D., Wiley-Livingston, C. A. & Levinson, S. R. (1982) in *Structure and Function in Excitable Cells*, eds. Chang, D., Tasaki, I., Adelman, W., Jr., & Leuchtag, H. (Plenum, New York), in press.
28. Miller, J. A., Levinson, S. R., Agnew, W. S. & Ellisman, M. H. (1982) *Biophys. J.* **37**, 385 (abstr.).
29. Beneski, D. A. & Catterall, W. A. (1980) *Proc. Natl. Acad. Sci. USA* **77**, 639–643.
30. Einarson, B., Gullick, W., Contri-Tronconi, B., Ellisman, M. & Lindstrom, J. (1982) *Biochemistry*, in press.